Gp135/podocalyxin and NHERF-2 participate in the formation of a preapical domain during polarization of MDCK cells

Doris Meder, Anna Shevchenko, Kai Simons, and Joachim Füllekrug

Max Planck Institute of Molecular Cell Biology and Genetics, D-01307 Dresden, Germany

Epithelial polarization involves the segregation of apical and basolateral membrane domains, which are stabilized and maintained by tight junctions and membrane traffic. We report that unlike most apical and basolateral proteins in MDCK cells, which separate only after junctions have formed, the apical marker gp135 signifies an early level of polarized membrane organization established already in single cells. We identified gp135 as the dog orthologue of podocalyxin. With a series of domain mutants we show that the COOH-terminal PSD-95/ Dlg/ZO-1 (PDZ)–binding motif is targeting podocalyxin to the free surface of single cells as well as to a subdomain of the terminally polarized apical membrane. This special localization of podocalyxin is shared by the cytoplasmic PDZ-protein Na$^+$/H$^+$ exchanger regulatory factor (NHERF)-2. Depleting podocalyxin by RNA interference caused defects in epithelial polarization. Together, our data suggest that podocalyxin and NHERF-2 function in epithelial polarization by contributing to an early apical scaffold based on PDZ domain-mediated interactions.

Introduction

Polarization is a feature of virtually all eukaryotic cells, creating an asymmetric distribution of plasma membrane proteins and lipids, the cytoskeleton, subcellular organelles, and intracellular transport pathways. In most cells, polarization occurs transiently in response to signals. However, columnar epithelia of organs like the kidney, intestine, or pancreas establish a terminally polarized monolayer in which they segregate an apical membrane facing the lumen from a basolateral membrane domain contacting other cells and the extracellular matrix. The identity of these membrane domains is maintained by the junctional complex, a diffusion barrier assembled with the help of PSD-95/Dlg/ZO-1 (PDZ)–based protein complexes (Bilder et al., 2003; Nelson, 2003; Roh and Margolis, 2003) and by intracellular sorting of membrane components (Le Gall et al., 1995; Mostov et al., 2003). Sorting of proteins and lipids can occur by targeted delivery and is achieved by segregating cargo according to sorting determinants, i.e., basolateral sorting motifs in the cytoplasmic tail of transmembrane proteins and

glycosylation or raft association for apical delivery, which are interpreted by sorting receptors either in the trans-Golgi network or in endosomes. A second sorting mechanism is selective retention in the target membrane domain (Matter and Mellman, 1994; Yeaman et al., 1999; Mellman and Warren, 2000).

Live microscopy suggests that polarized delivery of membrane proteins does not occur in single cells attached to the substratum; both apical and basolateral cargo is targeted to the basal surface. Only after establishing cell–cell contacts, basolateral cargo is routed to the top of the lateral membrane and apical cargo to the free surface (Kreitzer et al., 2003). There are two reasons for this observation. First, the exocyst, a protein complex specifically receiving basolateral cargo, is recruited to sites of cell–cell contact after cadherin-mediated cell adhesion (Grindstaff et al., 1998). Second, cell–cell contacts are the prerequisite for the assembly of the apical junctional complex, and junction formation is thought to precede polarized membrane traffic (Nelson, 2003). However, there is also evidence for polarized traffic of membrane proteins independent of functional apical junctions. During the cellularization process of *Drosophila melanogaster* embryos, the apical membrane is inserted from an intracellular pool at a time when no junctions have yet been established (Lecuit and Wieschaus, 2000). How, in this case, the apical membrane domain is held together until the apical adherence junctions are formed is not clear. In MDCK cells there is also evidence for membrane

polarization in the absence of cell–cell junctions. Viruses have been shown to bud out in a polarized fashion from single attached MDCK cells: influenza virus budded from the free surface whereas vesicular stomatitis virus was released basally (Rodriguez-Boulan et al., 1983). Recently it has been demonstrated that single intestinal epithelial cells could be induced to form an actin cap through activation of the kinase LKB1 (Baas et al., 2004).

Guided by the hypothesis that epithelial polarization might start with the formation of an apical pole in single cells, we studied the formation of the apical plasma membrane in MDCK cells. The most often used apical marker protein in studies on the polarization of MDCK cells is gp135, a transmembrane antigen linked to the cytoskeleton (Ojakian and Schwimmer, 1988). When MDCK cell cysts or sheets are induced to inverse their polarity by collagen overlays or during tube formation, gp135 is rapidly removed from the apical membrane and degraded to reappear by new synthesis at its new location (Ojakian et al., 1997; Pollack et al., 1998; Wang et al., 1990). Thus, gp135 invariably marks the apical lumen and it even showed a polarized distribution in MDCK cell monolayers prevented from forming tight junctions (Ojakian and Schwimmer, 1988).

In this work, we identify gp135 as podocalyxin. Furthermore, we provide the first evidence that a preapical scaffold is established already at the single cell stage and that it could function as the counterpart to the basal attachment site during early epithelial polarization of MDCK cells.

Results

Early polarity of gp135

To study early epithelial polarization, we seeded MDCK cells at low densities and followed apical and basolateral marker proteins by indirect immunofluorescence. We focused on the single cell and island stages at 1 and 4 h after plating, respectively. None of our apical or basolateral marker proteins displayed a polarized distribution at these stages. Apical GPI-anchored placental alkaline phosphatase (PLAP) and glycoprotein gp114 (influenza hemagglutinin, ICAM-1, and prominin are not depicted), as well as basolateral β1-integrin and E-cadherin (glycoprotein gp58 is not depicted), distributed all over the plasma membrane, with E-cadherin becoming enriched at sites of cell–cell contacts in islands of cells (Fig. 1, B and C). Only glycoprotein gp135 (Ojakian and Schwimmer, 1988) showed a polarized localization already at the single cell stage 1 h after plating. Staining for gp135 was exclusively on the free surface of MDCK cells, being absent not only from the basal membrane but also from the areas of membrane ruffling at the edge of the cell (Fig. 1 B). The distinct localization was not a remnant of apical-basal polarity before trypsinization because gp135 distributed evenly over the entire apical membrane at the starting point of our analysis (Fig. 1 A).

The early polarization of gp135 is unlikely to be due to biosynthetic trafficking because it occurred independently of ongoing protein synthesis as indicated by cycloheximide treatment (Fig. S1 A, available at http://www.jcb.org/cgi/content/full/jcb.200407072/DC1). Inhibition of endocytosis by expres-

sion of dominant-negative dynamin did not change the distribution of gp135 either (Fig. S1 B), suggesting that endosomal membrane sorting does not play a major role in the formation of this preapical pole. We also have no indication for the involvement of the vacuolar apical compartment that is reported to function as a storage compartment for apical proteins in cells cultured without calcium (Cohen and Musch, 2003). Because we observe gp135 at the cell surface at all times, diffusion in the plasma membrane rather than trafficking between subcellular compartments might be the predominant mechanism for sorting gp135 to the free surface of single cells. However, especially cells that were detached with trypsin sometimes showed intracellular accumulation of gp135 that partially colocalized with rab11-positive endosomes, indicating that some gp135 is subjected to endocytic recycling (Fig. S1 D).

The localization of gp135 remained distinct from other apical proteins throughout the polarization process. At the island stage, gp135 was absent from sites of cell–cell contact (Fig. 1 C), again in contrast to all other proteins analyzed. This was before the tight junction proteins occludin and claudin became enriched at lateral membranes (Fig. 1 C).

In terminally polarized MDCK cells, gp135 was localized to a subdomain of the apical plasma membrane. An area of 1.2–1.8 μm in diameter at the center of the apical membrane, as well as the outer rim close to the tight junctions, was devoid of gp135 staining (Fig. 1 D). In contrast, PLAP staining covered the whole apical region except a small exclusion area at the center. This central exclusion area corresponds to the site of outgrowth of the primary cilium (Fig. 1 E).

Our findings are schematized and summarized in Fig. 1 F. The aforementioned experiments reveal that the polarized distribution of gp135 precedes apical-basal polarity, and could thus reflect a so far uncharacterized early level of membrane organization during cell polarization.

Identification of gp135 as dog podocalyxin

Gp135 is a glycoprotein of unknown identity (Ojakian and Schwimmer, 1988), which we characterized as carrying both N- and O-linked glycans (Fig. S2, available at http://www.jcb.org/cgi/content/full/jcb.200407072/DC1). The protein was solubilized by Triton X-100 and enriched by lectin affinity chromatography (Fig. 2 A). Preparative immunoprecipitation from WGA-eluted fractions yielded a Coomassie band of the expected molecular mass (Fig. 2 B).

Analysis of tryptic peptides by nanoelectrospray tandem mass spectrometry produced several peptide sequence proposals (Table S1, available at http://www.jcb.org/cgi/content/full/jcb.200407072/DC1). An MS BLAST search confidently hit four mammalian podocalyxin proteins, although only one among the seven podocalyxin peptides was an exact match.

The cDNA sequence of dog podocalyxin was obtained by PCR of an MDCK cDNA library, starting with primers based on nucleotide homologies of known mammalian podocalyxin proteins. The corresponding amino acid sequence is shown in Fig. S3 (available at http://www.jcb.org/cgi/content/full/jcb.200407072/DC1) and exactly matches the peptide sequences obtained by mass spectrometry. Alignment of mammalian
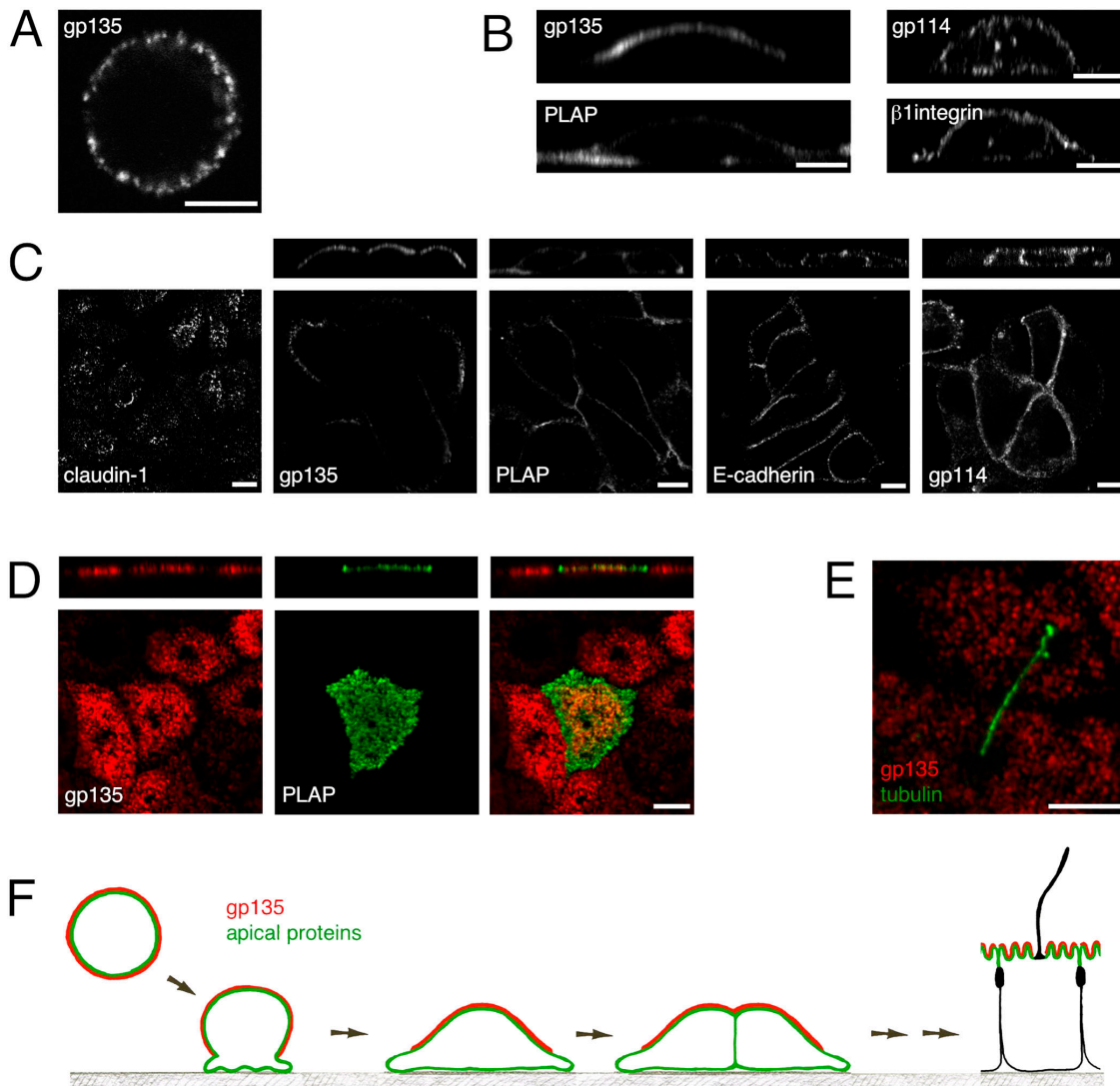
Figure 1. **Gp135 marks a specialized apical domain in MDCK cells.** PLAP-expressing MDCK cells were detached, fixed in suspension (A) or after plating onto coverslips (B, 1 h; C, 4 h), and stained with antibodies against apical (gp135, PLAP, and gp114) and basolateral (β1-integrin and E-cadherin) marker proteins. (A) Gp135 is distributed evenly over the whole surface of freshly detached and resuspended MDCK cells. (B) In single attached cells, gp135 is restricted to a preapical pole whereas other apical and basolateral marker proteins are not polarized. (C) Side views and confocal midsections of cell islands demonstrate that gp135 antibodies stain only the free surface, whereas PLAP, gp114, and E-cadherin are distributed randomly and localize to cell–cell contacts. The tight junction protein claudin-1 is still intracellular. Side views are merges of five vertical sections of confocal stacks. (D) Gp135 (red) is excluded from the center and the outer rim of the apical membrane of terminally polarized MDCK cells, whereas PLAP (green) is distributed over the entire apical membrane with only a small exclusion area in the center. Shown are confocal sections acquired from the same plane of the apical plasma membrane. (E) The exclusion area in the center of the apical membrane (gp135, red) corresponds to the site of outgrowth of the primary cilium as visualized by tubulin staining (green). Shown is a merged image of confocal sections taken of the apical membrane and the region above. Bars, 5 μm. (F) Overview of gp135 localization during the polarization of MDCK cells. Single, resuspended MDCK cells display an even distribution of plasma membrane proteins. Upon contact with a solid support, the cells establish a dynamic basal perimeter that includes apical membrane proteins (green) but not gp135 (red). When the cells flatten out and migrate toward each other, the basal plasma membrane and the edges of migrating cells are devoid of gp135. Upon cell–cell contact, gp135 disappears from the contacting membranes while other apical proteins remain. Apical-basolateral segregation starts at around 24 h and is completed after 3 d. In terminally polarized cells, gp135 is confined to a subdomain of the apical membrane that excludes the outer rim and the center surrounding the site of outgrowth of the primary cilium. Note that the membrane of the primary cilium (black) is devoid of classical apical marker proteins.

podocalyxin proteins (Kershaw et al., 1997; Takeda et al., 2000) including the dog homologue shows a highly conserved COOH-terminal part comprising the transmembrane domain and the cytoplasmic tail with its COOH-terminal Asp-Thr-His-Leu (DTHL) PDZ-binding motif. The extracellular NH2-terminal part features a conserved tetracysteine (C4) motif next to the transmembrane domain and a functionally conserved large O-glycosylated mucin domain.

Polarization and sorting of podocalyxin domain mutants

Podocalyxin/gp135 showed a localization strikingly different from other apical membrane proteins during early stages of MDCK cell polarization. To investigate which molecular modules are responsible for this difference, we constructed a series of expression plasmids (Fig. 3). Epitope-tagged podocalyxin showed the same localization as endogenous podocalyxin at all
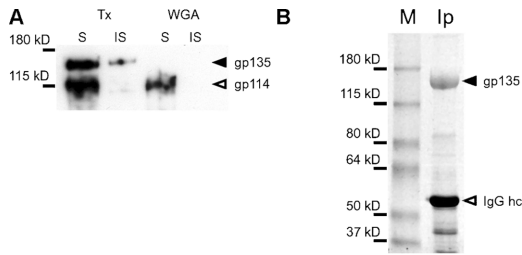
Figure 2. **Purification of gp135.** (A) Characterization of gp135 for enrichment from MDCK cells. Treatment with the nonionic detergent Triton X-100 and 1 mM EDTA on ice solubilized the majority of gp135 (S). Soluble and insoluble (IS) fractions were analyzed for their binding to wheat germ agglutinin (WGA). Shown is the analysis of the unbound fraction. All of gp135 is retained on the WGA column, whereas gp114 binds only partially. (B) Coomassie stained gel for identification of gp135. MDCK cells were treated with nonionic detergent on ice and solubilized glycoproteins enriched on a WGA column. Immunoprecipitation with mAbs against gp135 yielded a band at 135 kD. IgG hc corresponds to the heavy chain.

Figure 3. **Overview of podocalyxin domain mutants.** sstag, signal sequence followed by VSV-G epitope tag; mucin, Ser-Thr rich O-glycosylated domain; C4, tetracysteine stem region; TMD, transmembrane domain; cyt. tail, cytoplasmically oriented tail; DTHL, Asp-Thr-His-Leu COOH-terminal amino acids; gl-GFP, GFP containing two N-glycosylation sites; pcx, epitope tagged full-length podocalyxin; pcx-Δct, deletion of COOH-terminal DTHL motif; pcx-Δtail, deletion of cytoplasmic tail; pcx-GPI, GPI-anchored podocalyxin extracellular domain; pcx-ecto, soluble podocalyxin extracellular domain; GFP-tail, extracellular GFP with podocalyxin transmembrane domain and cytoplasmic tail; GFP-Δct, GFP-tail without COOH-terminal DTHL.

stages of polarization, but the deletion mutants often exhibited a less restricted distribution.

In single, freshly attached cells, pcx-GPI and pcx-Δct were found in the basal processes devoid of endogenous podocalyxin (Fig. 4, A and B), indicating that the COOH-terminal PDZ-binding motif contributes to the restricted localization. At the island stage, pcx-GPI was the only construct that distributed over the whole plasma membrane (Fig. 4, C and D), which points to a role for the transmembrane domain in keeping podocalyxin away from cell–cell contacts.

In terminally polarized MDCK cells, pcx-Δct, pcx-Δtail, and pcx-GPI displayed an unrestricted distribution over the entire apical surface. Pcx-GPI was even enriched in the regions devoid of endogenous podocalyxin (Fig. 4 E). Furthermore, both constructs were present in the membrane of the primary cilium, which could be visualized 1 μm above the plane of the apical surface (Fig. 4 E, insets). This finding suggests that the restricted apical localization of podocalyxin mostly depends on the four COOH-terminal amino acids.

Because all constructs evaluated so far (pcx, pcx-Δct, pcx-Δtail, and pcx-GPI) were apically targeted in terminally polarized cells, we generated additional constructs to assess the apical sorting determinants. The soluble extracellular domain of podocalyxin (pcx-ecto) was secreted predominantly to the apical side (Fig. 5 A), indicating the existence of an apical sorting signal in this region. To pinpoint other independent sorting determinants, we substituted the ectodomain with glycosylated GFP. GFP-Δct, containing the podocalyxin transmembrane domain and the cytoplasmic tail but lacking the four COOH-terminal amino acids, appeared poorly polarized and also accumulated intracellularly (Fig. 5, B and C). GFP-tail comprising the complete cytoplasmic tail was significantly more apical than GFP-Δct, indicating that the PDZ-binding motif also contributes to an efficient apical localization.

Podocalyxin depletion by RNA interference (RNAi)

Podocalyxin knockout mice die of kidney failure shortly after birth (Doyonnas et al., 2001). We were interested in the consequences of podocalyxin depletion in MDCK cells. Using a
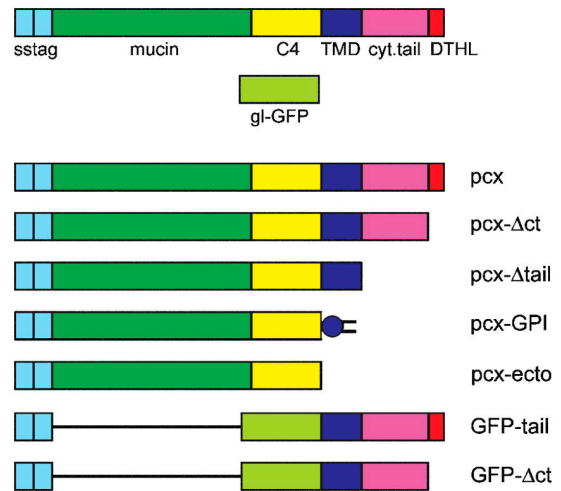
retrovirus-mediated small hairpin RNAi expression strategy (Schuck et al., 2004), we could knockdown podocalyxin mRNA in MDCK cells by 85–95% (real-time PCR), corresponding to ≤10% of wild-type protein levels (Fig. 6 A).

Podocalyxin-depleted cells grew much slower than control cells, increasing at only half the rate compared with control cells (Fig. 6 B). Polarization of knockdown cells was assayed by seeding them on filters at low densities, giving rise to a confluent monolayer after 24 h. Knockdown cells grown on filters for 2 d showed a delay in polarization when compared with control cells (Fig. 6 C). Podocalyxin-depleted cells occupied a larger surface area (292 ± 60 μm^2) but were not as tall (5.8 ± 0.5 μm) as control cells (103 ± 18 μm^2 and 8.6 ± 0.4 μm). The basolateral marker protein gp58 showed an unpolarized distribution in knockdown cells but was properly localized on control filters. Similarly, the apical marker proteins gp114 and PLAP appeared less polarized.

The same knockdown phenotype was obtained with three different target sequences, but to prove that it was specifically due to the lack of podocalyxin, we performed rescue experiments using MDCK cells stably expressing a GFP-tagged podocalyxin resistant to our hairpin sequence. Depletion of endogenous podocalyxin protein by >90% in the GFP-pcx–expressing cells did not result in the severe phenotype of similarly depleted wild-type cells (Fig. 7). GFP-pcx–expressing knockdown cells occupied a similar surface area as control cells (control: 84 ± 17 μm^2, knockdown: 311 ± 127 μm^2, knockdown+GFP-pcx: 108 ± 24 μm^2) and were only slightly shorter (control: 12.3 ± 0.7 μm, knockdown: 6.5 ± 1.3 μm, knockdown+GFP-pcx: 9.4 ± 0.7 μm), which might be due to the heterogeneous and possibly lower expression of GFP-pcx compared with endogenous podocalyxin.
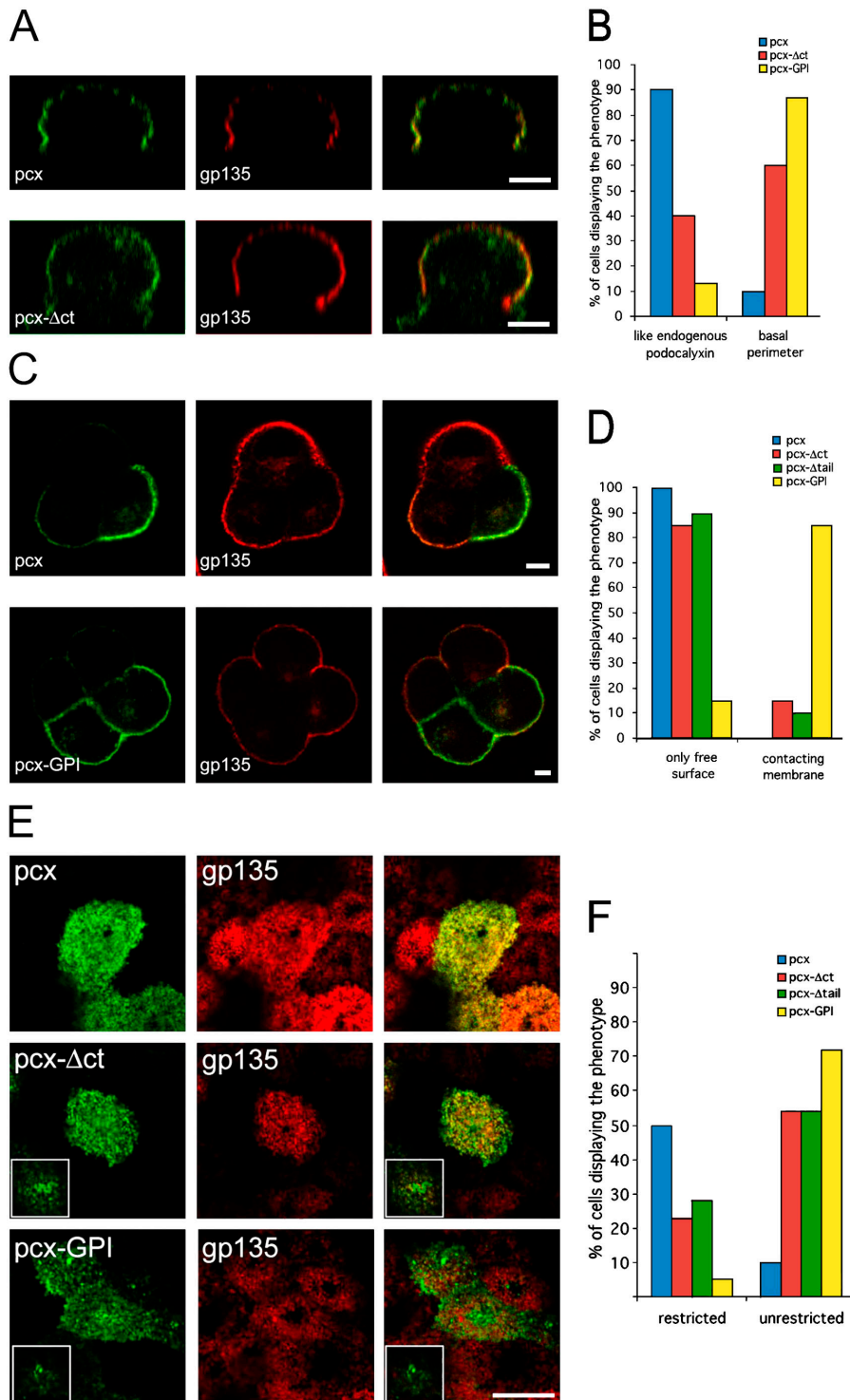
Figure 4. **Localization of podocalyxin domain mutants.** (A) Transiently transfected MDCK cells were analyzed 1 h after seeding. Epitope-tagged podocalyxin (pcx) colocalized to a high degree with endogenous podocalyxin, with both proteins being restricted to the free surface above the attachment area (top). In contrast, the domain mutant proteins often also localized to the dynamic basal perimeter of the cell (pcx-Δct; bottom). Endogenous podocalyxin is stained with the anti-gp135 antibody (red), and the mutant proteins are stained with anti-VSVG-tag antibody (green). Vertical sections of confocal stacks. Bars, 5 μm. (B) Scoring of localization patterns in single cells. "Like endogenous podocalyxin" means excluded from the basal perimeter. "Basal perimeter" refers to the additional presence in the dynamic basal extensions. Note that none of the mutant proteins showed efficient staining of the membrane in contact with the substratum. (C) MDCK cells 4 h after seeding. Confocal midsections reveal either staining of the free surface only (pcx; top) or localization to both the free surface and the contacting membrane (pcx-GPI, bottom). Bars, 5 μm. (D) Scoring of localization patterns in islands of cells. A phenotype similar to endogenous podocalyxin was scored as "only free surface." Staining all over the plasma membrane was scored as "contacting membrane." Pcx-GPI localizes to all plasma membrane domains. (E) Analysis of filter grown cells. Epitope-tagged podocalyxin (pcx) is excluded from the center region of the apical surface like endogenous podocalyxin. Pcx-Δct and pcx-GPI are also present on the ciliary membrane (insets). Note that pcx-GPI is even segregated from endogenous podocalyxin. Shown are confocal sections of the apical region of MDCK cells. The insets for pcx-Δct and pcx-GPI are taken from the central cell, 0.92 μm above the apical membrane. Bar, 10 μm. (F) Scoring of the restricted localization. A phenotype similar to endogenous podocalyxin is classified as "restricted," and an unrestricted localization for the expressed mutant protein as "unrestricted." The remaining percentage of transfected cells did not show an exclusion area for endogenous podocalyxin.

To investigate whether the primary defect of the knockdown cells was cell growth or cell polarization, we studied cyst formation in a collagen matrix. In this case, single cells grow to form multicellular, polarized arrangements in the absence of a rigid substrate (Wang et al., 1990). After 4 d in culture, 78% of control cells had formed round cysts with one central lumen. At the same time, knockdown cells had formed cysts of similar size, but only 19% were correctly polarized toward one central cavity. 49% displayed multiple lumens and 32% did not form any lumen at all (Fig. 6 D). This result indicates that the main defect in knockdown cells is impaired polarization rather than slowed growth and that it predominantly afflicts apical membrane formation.

Na+/H+ exchanger regulatory factor (NHERF)-2 localization to the free surface of MDCK cells

The domain of podocalyxin contributing most definitely to both the early level of polarity of single cells and the restricted
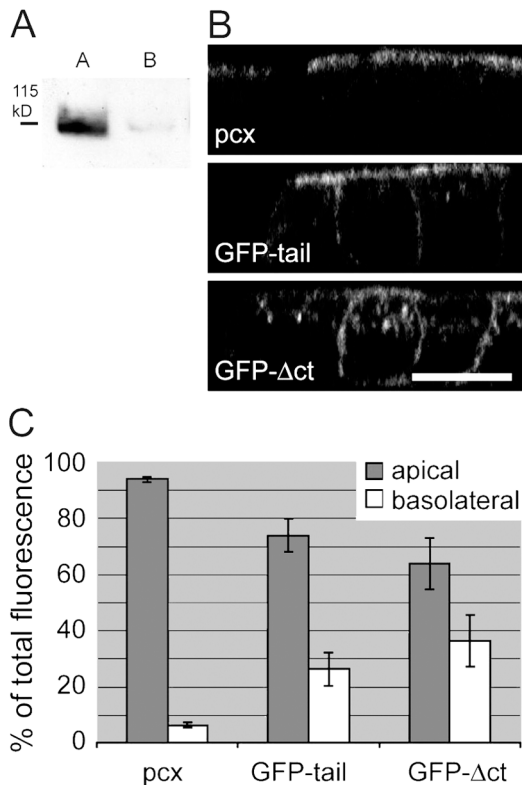
Figure 5. **Apical sorting determinants within podocalyxin.** (A) Polarized secretion of the soluble pcx-ectodomain. Terminally polarized, filter grown MDCK cells stably expressing pcx-ecto were analyzed by a secretion assay. Media supernatants were collected for 2 h. The apparent molecular mass of pcx-ecto is ∼110 kD. A, apical; B, basolateral. (B) Apical sorting of podocalyxin mutant proteins in stably expressing, terminally polarized cells. Depicted are epitope-tagged podocalyxin (pcx), GFP-tail, and GFP-Δct. GFP-tail lacking the extracellular domain of podocalyxin is still preferentially apical, whereas the corresponding protein without the four COOH-terminal amino acids appears unpolarized and partially intracellularly retained. Side views of polarized MDCK cell layers. Bar, 10 μm. (C) Quantification of apical and basolateral localization. Images were recorded so that the complete range of fluorescence intensities was included. Apical and basolateral membranes were outlined and fluorescence units calculated using Image J software. Relative apical and basolateral contributions were first calculated for individual cells and then for all cells of one population. Error bars are SD representing the variation of apical versus basolateral localization.

apical localization of terminally polarized cells is the COOH-terminal PDZ domain–binding motif. This motif has been shown to bind the cytoplasmic PDZ domain protein NHERF-2 (Takeda et al., 2001; Li et al., 2002).

We constructed a GFP fusion protein to follow the localization of NHERF-2 during development of polarity. Intriguingly, GFP-NHERF-2 localized similarly to podocalyxin in all stages of epithelial polarization. It was confined to the free surface in single cells and at the island stage (Fig. 8, A and B, apical gp114 and basolateral β1-integrin for comparison). In terminally polarized MDCK cells, GFP-NHERF-2 localized to the apical surface, where it was, like podocalyxin, excluded from the center signifying the area of outgrowth of the primary cilium (Fig. 8 C).

Coimmunoprecipitation experiments provided additional evidence for an interaction between NHERF-2 and podoca-

lyxin at early stages of polarization (Fig. 8 D). Moreover, the more confluent the cells become, the more podocalyxin is co-precipitated, indicating a maturation of the interaction as the cells differentiate toward terminal polarization.

Early polarization is thus not a unique peculiarity of podocalyxin, but a feature it shares with NHERF-2 and presumably other proteins.

Discussion

The mechanism of apical and basolateral domain formation during epithelial polarization is not understood. In this work, we wanted to pinpoint the first events leading to plasma membrane domain segregation. We found that the transmembrane protein podocalyxin and its cytoplasmic binding partner NHERF-2 marked a preapical domain already in single cells, and propose that PDZ-mediated interactions could create an early apical scaffold forming the counterpart to the basal attachment site in cells initiating epithelial polarization.

Gp135 is dog podocalyxin

Surprisingly, the most often used apical marker protein of MDCK cells turned out to be podocalyxin. This protein had first been identified in podocytes of the kidney glomerulus and later in endothelial cells and hematopoetic cells (Kerjaschki et al., 1984; Horvat et al., 1986; Kerosuo et al., 2004). However, no podocalyxin has been observed in the tubular cells of the nephron. As MDCK cells are thought to be derived from the collecting duct or the distal tubule (Cereijido et al., 1978), the expression program is obviously changed after immortalization and continuous culture. Recent studies have demonstrated that primary kidney cells immortalized by the adenoviral E1A gene started to express podocalyxin but were still well differentiated, nontransformed, and able to form tubules in Matrigel (Takeuchi et al., 2002).

Podocalyxin marks specialized apical domains in single cells and epithelia

Gp135/podocalyxin has been demonstrated to be a reliable marker of the apical membrane. We found at least two sorting determinants securing the apical localization of the protein, one in the ectodomain and one in the COOH terminus. The apical targeting of several membrane proteins has been reported to rely on PDZ-binding motifs and NHERF proteins (Shenolikar and Weinman, 2001; Voltz et al., 2001). Podocalyxin deleted of the COOH-terminal PDZ-binding motif has been reported to be less stable in the apical membrane (Li et al., 2002). Consistent with this finding, we see the COOH-terminally deleted podocalyxin mutant proteins pcx-Δct and GFP-Δct more in intracellular, vesicular structures than their full-length tail counterparts pcx and GFP-tail. However, the extracellular domain also contains sorting information because the soluble ectodomain is secreted apically. Furthermore, swapping the extracellular domain of podocalyxin for GFP resulted in a protein partially mislocalized to the basolateral membrane. This is in agreement with detailed analysis of the apical targeting of CFTR, which demonstrated that targeting of this protein is also not solely dependent on the
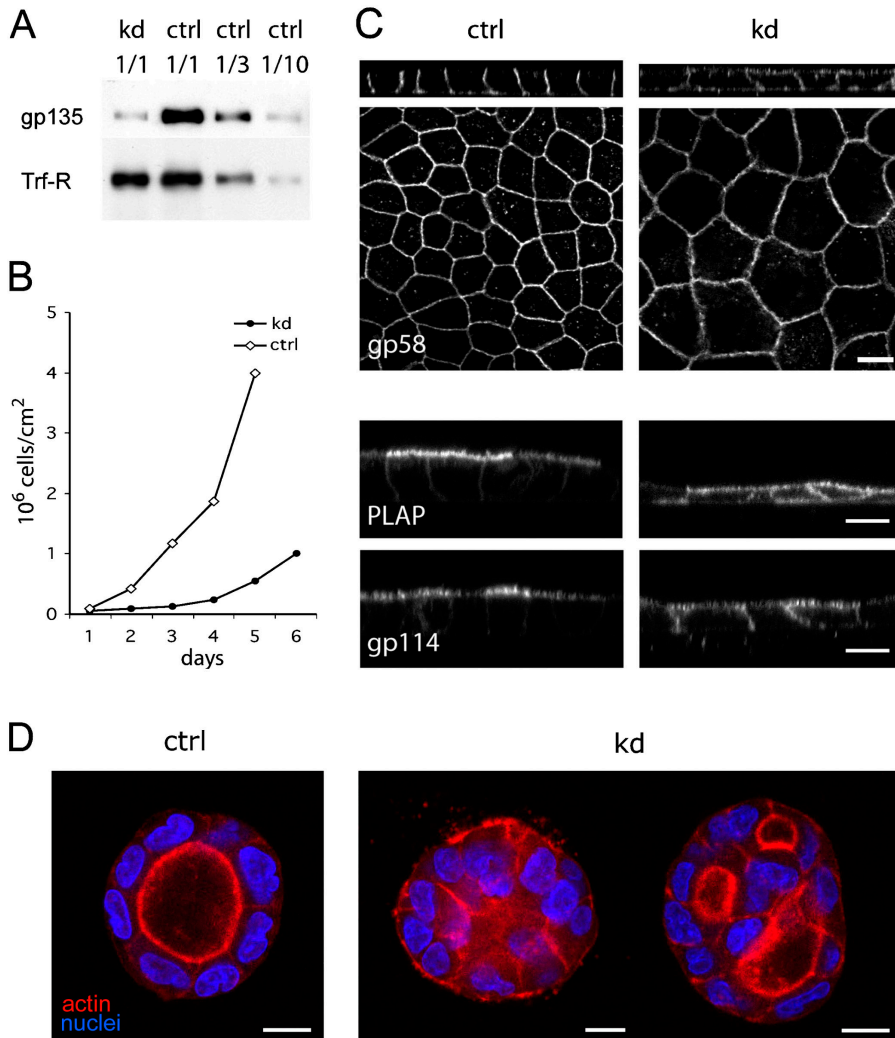
Figure 6. Podocalyxin knockdown by RNAi. (A) Knockdown efficiency for podocalyxin in MDCK cells. Total lysates (15 µg of protein) of knockdown cells (kd) were compared with lysates from control cells by Western blotting (ctrl; 1/1: 15 µg, 1/3: 5 µg, 1/10: 1.5 µg). Podocalyxin is reduced to ~10% of wild-type levels in knockdown cells. Transferrin receptor (Trf-R) serves as a loading control. (B) Growth retardation of podocalyxin knockdown cells. 50,000 cells were seeded into individual 10-cm² wells at day 0 and trypsinized cells counted each following day. Numbers of knockdown cells (kd) increased by an average of 1.7-fold per day in the first 4 d after seeding, whereas control cells (ctrl) multiplied at a rate of 3.2-fold per day. At 4×10^6 cells/10 cm² cells are confluent. (C) Immunofluorescence analysis of filter grown knockdown cells. Knockdown and control cells were seeded onto filters and fixed 2 d after reaching confluency. A confocal midsection stained for the basolateral marker gp58 shows that knockdown cells occupied a larger surface area. The corresponding vertical section shows that knockdown cells were less tall and did not restrict gp58 to the basolateral surface like control cells. The apical marker proteins gp114 and PLAP also displayed a less polarized distribution in knockdown cells. (D) Apical lumen formation in knockdown cells. Knockdown and control cells were suspended in Matrigel and cultured in the matrix for 4 d. Whereas >78% of the control cells had formed cysts with one central apical lumen as visualized by actin staining with Alexa Fluor 633-phalloidin and nuclear staining with DAPI, only 18% of knockdown cells displayed a single central lumen. 32% had no lumen and 50% displayed multiple small lumens. Bars, 10 µm.

PDZ motif (Swiatecka-Urban et al., 2002; Ostedgaard et al., 2003). Similarly, NHERF-1/EBP50 has lost its apical localization in the intestine of ezrin-deficient mice, but NHE3 is still properly targeted to the apical side (Saotome et al., 2004).

We found podocalyxin to localize to a subdomain of the apical membrane of terminally polarized MDCK cells. It was absent from the junctional perimeter of the apical membrane and from a large area in the center where the primary cilium emerged. Mutational analysis demonstrated that all podocalyxin constructs lacking the PDZ-binding motif invaded the exclusion region and the cilium. Consistent with this finding, GFP-tagged NHERF-2 was also excluded from the center region of the api-
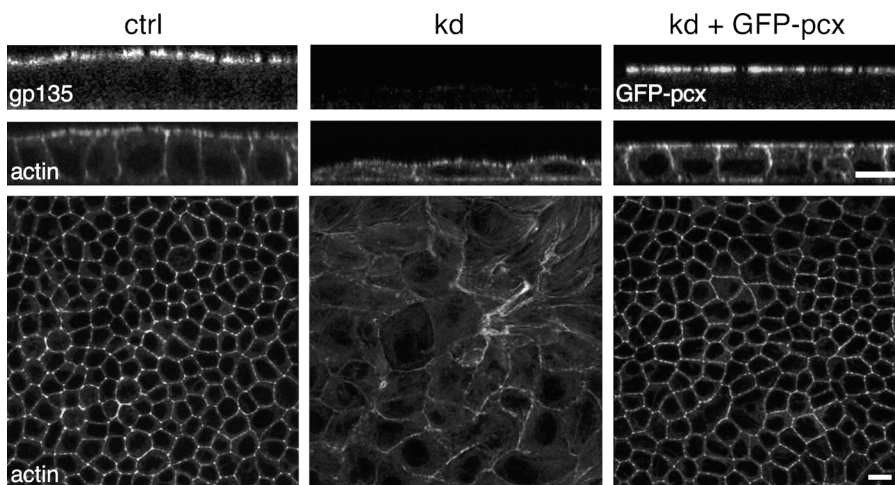

Figure 7. Rescue of the polarization defect in knockdown cells by expression of GFP-podocalyxin. Knockdown cells, control cells, and knockdown cells stably expressing RNAi-resistant GFP-podocalyxin were seeded onto filters and fixed 2 d after reaching confluency. TRITC-phalloidin staining of actin shows that the GFP-pcx–expressing knockdown cells occupy a surface area similar to control cells and that they were almost as tall as control cells. Bars, 10 µm.
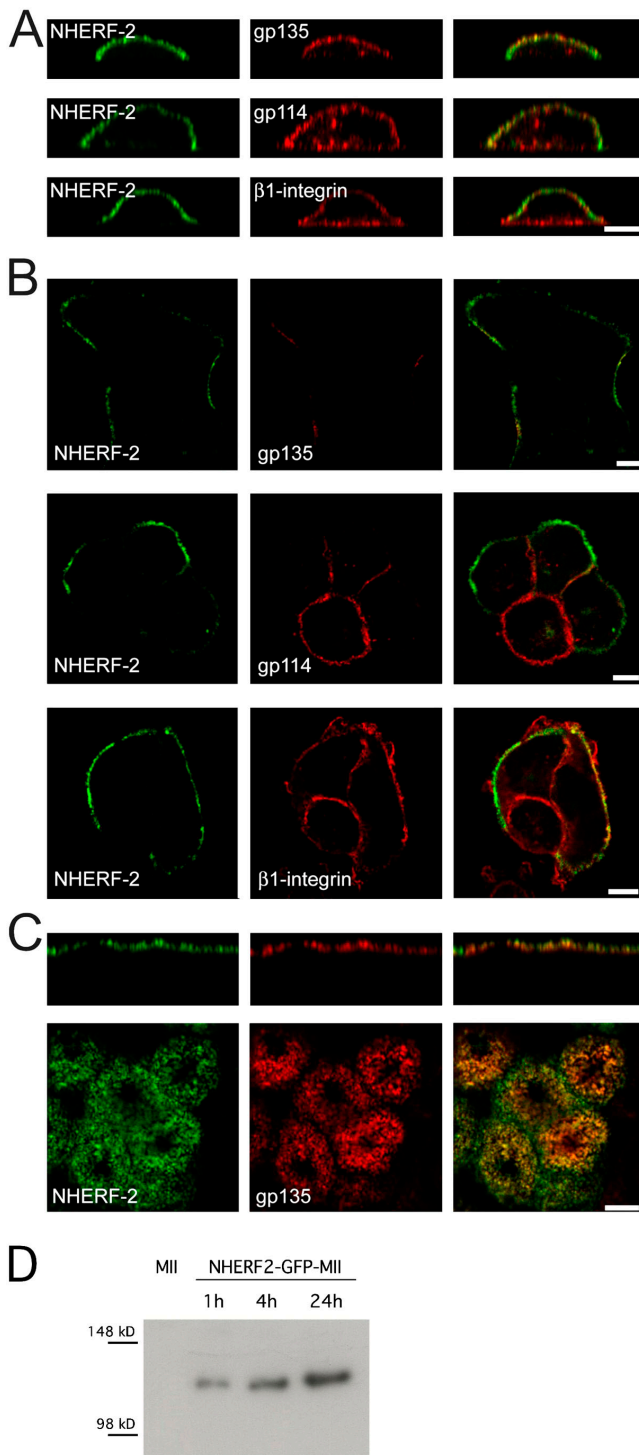
Figure 8. **NHERF-2 shows a restricted localization similar to podocalyxin.** MDCK cells stably expressing GFP-NHERF-2 were plated onto coverslips and fixed after 1 (A) and 4 h (B). (A) Side view of single cells. (B) Midsection through islands of cells viewed from the top. Both gp114 and β1-integrin show prominent staining of the contacting plasma membrane, whereas GFP-NHERF-2 and podocalyxin localize to the free surfaces surrounding the cell islands. Little GFP-NHERF-2 was observed at the cell–cell border. (C) Apical colocalization of GFP-NHERF-2 with podocalyxin in terminally polarized MDCK cells. Bars, 5 μm. (D) Interaction of podocalyxin and NHERF-2 at early stages of polarization. MDCK cells stably expressing GFP-NHERF-2 were allowed to attach for 1, 4, or 24 h. Postnuclear supernatants were immunoprecipitated with a GFP antibody. Western blotting with a podocalyxin antibody reveals increasing amounts from 1 to 24 h after seeding.

cal membrane. NHERF-2 binds ezrin/radixin/moesin family proteins, providing a link between plasma membrane proteins and the actin cytoskeleton (Bretscher et al., 2000; Voltz et al., 2001). A recent paper even links podocalyxin directly to ezrin (Schmieder et al., 2004). Interestingly, gp135 has been shown to be enriched in microvilli (Ojakian and Schwimmer, 1988), actin-based structures protruding from the apical membrane. Presumably, their interaction with the actin cytoskeleton prevents podocalyxin and NHERF from entering the ciliary membrane. The cilium outgrowth is one of the final events in the polarization of the MDCK cell layer (Bacallao et al., 1989). The source of the ciliary membrane is not known, but it is devoid of classical apical marker proteins. In contrast, membrane proteins involved in the pathogenesis of polycystic kidney disease are restricted to the ciliary membrane but absent from the rest of the apical surface (Pazour and Witman, 2003). These are intriguing examples of subcompartmentalization of the epithelial surface, which still remain poorly understood.

The most striking property of podocalyxin was that it localized exclusively to the free surface of single MDCK cells after plating, and this property was shared by NHERF-2. This polarized distribution stood in stark contrast to all other apical (and basolateral) marker proteins tested, which were instead found all over the plasma membrane. Overexpressing the kinase LKB1 and its activator STRAD in intestinal cells led to formation of an apical brush border on the free surface of single cells (Baas et al., 2004). This "actin cap" was enriched in apical marker proteins and surrounded by the junctional proteins ZO-1 and p120. Our case very likely represents an earlier or different polarization event because we do not observe a general concentration of apical proteins at the free surface of single cells, nor even at the island stage several hours after plating. Whether or not there are epithelial cells that establish an "actin cap" at the single cell stage of their normal differentiation remains to be seen. Genetic evidence implicates Par-proteins like LKB1 and especially the three polarity complexes Par3/Par6/aPKC/Cdc42/JAM, Crumbs3/Pals1/PatJ, and Dlg/Scribble/Lgl in epithelial polarization (Bilder et al., 2003; Hurd et al., 2003), but how the signaling events triggered by LKB1 or the interactions between the polarity complexes led to the formation of stable plasma membrane domains with distinct compositions and properties and to the redirection of membrane traffic is not fully understood.

A role for podocalyxin in epithelial polarization

The studies on the function of podocalyxin have focused on its role in the podocyte of the glomerulus. Podocalyxin is localized on the free surface of the podocyte foot processes and is thought to be involved in keeping the slit membranes open for filtration (Orlando et al., 2001). In podocalyxin knockout mice the podocytes fail to form foot processes and slit membranes and ultrafiltration in the glomerulus is blocked (Doyonnas et al., 2001). We wondered if podocalyxin is required for the formation of a functional MDCK cell layer. Using a retrovirus protocol to express hairpin RNAs, we have knocked down 13 proteins presumably involved in epithelial polarization

(Schuck et al., 2004). None of these proteins showed the striking polarization defect we report for the podocalyxin knockdown cells grown on semipermeable filters or in a collagen matrix. Podocalyxin-depleted cysts showed aberrant lumen formation as compared to the single central lumen formed by control cell cysts. The cyst experiment clearly defines a polarization defect that is independent of cell growth because in control cells also the small cysts display a single central cavity, whereas in knockdown cells even larger cysts can completely lack the apical lumen. We found the cysts to be a more sensitive indicator of polarization defects, probably because the establishment of a uniform polarization axis in the whole cell assembly within a three-dimensional collagen matrix is more complex than on a two-dimensional rigid support.

Polarization is known to be initiated by cues from the extracellular matrix or from cell–cell contacts, which then are responsible for establishing the basal sites that transmit signals to the microtubule and the actin networks. The signals are relayed to the secretory and endocytic apparatus to start the reorganization of the cytoplasm and the plasma membrane, which culminates in the establishment of stably polarized cells (Drubin and Nelson, 1996). Still, it is not obvious how a local cue affects the rearrangement of the entire cell. One suggestion involves the architectural principles of the tensegrity model in which constructions are held together by struts and elastic strings (Ingber, 2003a,b), corresponding to microtubules and actin filaments in a cell, respectively. A distortion at one end is likely to lead to compensatory processes in the whole network to ensure integrity of the overall architecture. Transferred to attaching epithelial cells this might mean that the counterpart to the basal attachment site could be the creation of an apical scaffold. Transmembrane proteins like podocalyxin that have COOH-terminal PDZ-binding motifs and PDZ proteins like NHERF are good candidates for forming this scaffold. These proteins include apical ion transporters (NHE3, sodium-phosphate cotransporter type IIa), the cystic fibrosis transmembrane conductance regulator CFTR (Voltz et al., 2001), and most importantly Crumbs3, a protein that is part of the apical polarity complex and the overexpression of which has been shown to delay tight junction formation in MDCK cells and cause aberrant cyst development (Roh et al., 2003). NHERF proteins contain two PDZ domains with different binding specificities and are able to dimerize or even oligomerize (Nourry et al., 2003). By binding to several members of the ezrin/radixin/moesin family of cytoskeletal adaptors, NHERF and other PDZ domain proteins could cross-link their multiple transmembrane ligands to form a preapical membrane platform scaffolded by the cytoskeleton. This platform could serve as a docking site for polarized membrane traffic and also signify the domain boundaries for junction formation. At the same time it could function as a regulatory device sending signals to integrate these processes with other events working toward epithelial polarization. How such integration is accomplished from the first external cues reaching an unpolarized cell to the events that follow to form a polarized epithelial cell layer, will be difficult to unravel. However, the idea that cell architecture and mechanistic regulation are linked by signaling networks is attractive. Podocalyxin could be one of the structural guideposts during this process.

Materials and methods

Antibodies
The hybridoma cell line 3F2 secreting antibodies against gp135 (Ojakian and Schwimmer, 1988) was provided by G. Ojakian (State University of New York Downstate Medical Center, Brooklyn, NY) and A. Muesch (Cornell University, Ithaca, NY). Antibodies against PLAP (Verkade et al., 2000), E-cadherin (Gumbiner and Simons, 1986), gp114, and gp58 (Balcarova-Stander et al., 1984) have been raised in our laboratory. Other antibodies used were as follows: mouse anti–β1-integrin (Chemikon International), rabbit anti–claudin-1 (Zymed Laboratories), rabbit anti–α-tubulin (Santa Cruz Biotechnology, Inc.), mouse anti-transferrin receptor (Zymed Laboratories), and goat anti-GFP (provided by D. Drechsel, Max Planck Institute of Molecular Cell Biology and Genetics, Dresden, Germany). Rabbit anti–VSV-G epitope tag was a gift from T. Nilsson (European Molecular Biology Laboratory, Heidelberg, Germany).

Purification of gp135
MDCK cells were collected in PBS, washed with TNE (20 mM Tris, pH 7.4, 150 mM NaCl, and 1 mM EDTA), and homogenized with ice-cold TNE containing 1% (wt/vol) Triton X-100. After incubation on ice for 30 min, the solution was adjusted to WGA buffer (10 mM Hepes, pH 7.4, 1 mM MgCl$_2$, 1 mM CaCl$_2$, 150 mM NaCl, and 0.1% Triton X-100) and insoluble material was sedimented for 1 h at 100,000 g. The supernatant (120 mg of protein) was circulated overnight over a 5-ml WGA-agarose (Amersham Biosciences) column. Glycoproteins were eluted with 0.3 M N-acetylglucosamine in WGA buffer, concentrated in spin columns (model Centrikon YM-30; Millipore), and the final yield was 0.45 mg of protein.

For immunoprecipitation, the solution was adjusted to pH 6.0 with 1 M of potassium phosphate buffer and 12 μg IgG was added. After incubation for 2 h at RT, IgG were collected with protein G–Sepharose and washed, and bound proteins were solubilized in SDS gel sample buffer, separated by SDS-PAGE, and visualized by Coomassie staining.

The identification of gp135 by mass spectrometry is provided in the online supplemental material.

Podocalyxin domain constructs and NHERF2-GFP
A detailed description of the cloning of dog podocalyxin is provided in the online supplemental material. All cDNA sequences were constructed by PCR, subcloned into the expression vector pcDNA3, and sequenced for verification. The NH$_2$ terminus always comprised a signal sequence epitope tag cassette composed of the signal sequence of human CD8α (MALPVTALLLPLALLLH-AARP) and the VSV-G epitope tag P5D4 (YTDIEMN-RLGK). The mucin domain–containing constructs are based on rabbit podocalyxin cDNA (provided by D. Kershaw, University of Michigan, Ann Arbor, MI; Kershaw et al., 1995). PCR products were digested with ClaI and NotI, and cloned into ss-tag-pcDNA3 containing the signal sequence and the first half of the epitope tag. Primers used were as follows: pcx (s-rb, α-sN), pcx-Δct (s-rb, α-nP), pcx-Δtail (s-rb, α-notail), and pcx-ecto (s-rb, α-gpi). Removal of the stop-linker sequence in pcx-ecto and replacement with the sequence coding for attachment of a GPI anchor from CD58 (P19256; amino acids 207–237) obtained as a BamHI–NotI fragment from pN1-FcRGPI (Keller et al., 2001) yielded pcx-GPI. Glycosylated GFP was constructed by PCR with primers sET-GFP and α-glyc. A pcx-Δmuc construct lacking the mucin domain was obtained directly by PCR of the MDCK cDNA library using primers s-muc and α1. Fusion proteins with glycosylated GFP in place of the podocalyxin ectodomain were derived from pcx-Δmuc by PCR with primers s-EDRF and α-sN, α-nP, α-notail, and contain GFP followed by a 16-aa glycosylation tag from human rhodopsin (NGTEGPNFYVPFSNAT; Bulbarelli et al., 2002). Rabbit-pcx was incorporated into this GFP plasmid as an EcoRI–NotI fragment yielding GFP-pcx. All oligonucleotide sequences are supplied in Table S2 (available at http://www.jcb.org/cgi/content/full/jcb.200407072/DC1).

NHERF-2 cDNA (provided by R. Hall, Emory University School of Medicine, Atlanta, GA) was cut out by restriction digest with EcoRI and KpnI, and ligated into plasmid pEGFP-C2 (BD Biosciences), resulting in a fusion protein with NH$_2$-terminal GFP and COOH-terminal NHERF-2.

Cell culture, transfection, and secretion assay
MDCK II and PLAP-MDCK (provided by D. Brown, State University of New York, Stony Brook, NY) cells were grown in MEM with 5% FCS. Cells

were detached by incubation in Trypsin/EDTA (Invitrogen) or without trypsin by treatment with 1 mM EDTA after overnight culture in low-calcium MEM with dialyzed FCS. No difference in localization for any protein was observed, but staining efficiency for podocalyxin was improved when omitting trypsin (Ojakian et al., 1990). For terminal polarization, cells were seeded on Transwell filters (Corning Costar) in MEM, 10% FCS, and cultured for 4 d. MDCK cells were transfected by electroporation (5 μg DNA for 10^6 cells; Amaxa Technology). Stably transfected pools of MDCK cells were generated by selection with 0.5 mg/ml G-418 for 2 wk.

For evaluation of polarity of secretion, the podocalyxin-ectodomain–expressing pool of MDCK cells was cultivated for 4 d on Transwell filters, washed with low-protein tissue culture medium without FCS (Opti-MEM; Invitrogen), and incubated for 2 h with 500 μl of Opti-MEM for the apical and basolateral chamber each. Supernatants were clarified from debris, precipitated, and analyzed by gel electrophoresis and Western blotting.

Immunofluorescence microscopy

Immunofluorescence was performed as described previously (Füllekrug et al., 1999) using FITC-, Cy3-, or Cy5-coupled secondary antibodies (Dianova). Confocal microscopy was done at RT on a microscope (model LSM 510; Carl Zeiss MicroImaging, Inc.) and a TCS SP2 system (Leica; 63× oil immersion objectives, NA 1.4). Double immunofluorescence images were taken sequentially, and parameters were adjusted so that all light intensities were in the recording range. Confocal stacks were acquired with a slice thickness of 300 nm.

Micrographs were derived as indicated in the figure legends from single confocal planes, several merged confocal planes, vertical sections generated from confocal stacks with the LSM software (Carl Zeiss MicroImaging, Inc.), or as a merged image of several vertical sections generated by reslicing of a confocal stack with Image J software (W. Rasband, National Institutes of Health, Bethesda, MD). Pictures were arranged with Adobe Photoshop and Adobe Illustrator.

For scoring of domain mutant constructs and quantification of apical/basolateral distribution see the online supplemental material. Cell heights and surface area were measured manually using the LSM software.

RNAi

Hairpin-forming oligonucleotides targeting a sequence of 19–21 nucleotides (pcx5a and pcx5s, pcx7a and 7s, and pcx9a and pcx9s; Table S2) were incorporated into retroviruses as recently described from our laboratory (Schuck et al., 2004). With all three target sequences, depletion of mRNA levels reached 85–95% at day 4 after transduction, protein levels were down to 10% between day 6 and 9 after transduction, but both mRNA and protein levels increased rapidly after day 10. Therefore, the residual amount of podocalyxin protein was determined at the day of the experiment for every knockdown, and only those with a knockdown ≥90% were analyzed for phenotypes. To keep podocalyxin levels down more consistently, retroviral transduction was in some experiments combined with transfection of RNAi plasmid. Control plasmids contained hairpin sequences that were not effective.

For rescue experiments, a pool of MDCK cells stably expressing a GFP-podocalyxin chimera containing the ectodomain of rabbit-podocalyxin and the transmembrane domain and cytoplasmic tail of the dog homologue was transduced with the pcx7 RNAi sequence targeting the NH_2-terminal portion of the dog sequence.

For polarization analysis, 10^5 cells were seeded onto transparent 12-mm transwell filters and analyzed by immunofluorescence after 2 d. For cyst formation, 25 μl of cell suspension containing 50,000 cells were mixed with 50 μl of growth factor–reduced Matrigel (Becton Dickinson), 12-μl drops were placed into 2-cm² wells and allowed to solidify for 1 h at 37°C before culture medium was added. After 4 d in culture with daily medium changes, most of the control cells had formed cysts with a single apical lumen.

Coimmunoprecipitation

MDCK cells stably expressing GFP-NHERF2 were extracted with 1% Triton X-100 in TNE on ice for 30 min, and unsolubilized membranes were removed by centrifugation at 100,000 g. The supernatant was incubated at 4°C with a polyclonal anti-GFP antibody bound to protein A–Sepharose. Beads were washed with TNE/0.5% Triton X-100, and bound proteins were eluted by boiling in sample buffer. After SDS-PAGE and Western blot, the membranes were developed with the monoclonal gp135 antibody.

Online supplemental material

Fig. S1 illustrates that the sorting of gp135 to the preapical pole is independent of ongoing protein synthesis and endocytosis, although some gp135 is subjected to endocytic recycling as it localizes to rab11-positive structures. Fig. S2 shows that gp135 is N- and O-glycosylated. Fig. S3 is an alignment of the protein sequence of dog podocalyxin with its mammalian orthologues. Table S1 displays the identification of gp135 by tandem mass spectroscopy and MS BLAST searching. Table S2 gives the sequences of all oligonucleotides used for cloning. Detailed information on the cloning of dog podocalyxin can be found in the legend to Fig. S3. Supplemental Materials and methods gives information on the scoring and quantification of immunofluorescence experiments. Online supplemental material is available at http://www.jcb.org/cgi/content/full/jcb.200407072/DC1.

References

Baas, A.F., J. Kuipers, N.N. van der Wel, E. Batlle, H.K. Koerten, P.J. Peters, and H.C. Clevers. 2004. Complete polarization of single intestinal epithelial cells upon activation of LKB1 by STRAD. *Cell.* 116:457–466.

Bacallao, R., C. Antony, C. Dotti, E. Karsenti, E.H. Stelzer, and K. Simons. 1989. The subcellular organization of Madin-Darby canine kidney cells during the formation of a polarized epithelium. *J. Cell Biol.* 109:2817–2832.

Balcarova-Stander, J., S.E. Pfeiffer, S.D. Fuller, and K. Simons. 1984. Development of cell surface polarity in the epithelial Madin-Darby canine kidney (MDCK) cell line. *EMBO J.* 3:2687–2694.

Bilder, D., M. Schober, and N. Perrimon. 2003. Integrated activity of PDZ protein complexes regulates epithelial polarity. *Nat. Cell Biol.* 5:53–58.

Bretscher, A., D. Chambers, R. Nguyen, and D. Reczek. 2000. ERM-Merlin and EBP50 protein families in plasma membrane organization and function. *Annu. Rev. Cell Dev. Biol.* 16:113–143.

Bulbarelli, A., T. Sprocati, M. Barberi, E. Pedrazzini, and N. Borgese. 2002. Trafficking of tail-anchored proteins: transport from the endoplasmic reticulum to the plasma membrane and sorting between surface domains in polarised epithelial cells. *J. Cell Sci.* 115:1689–1702.

Cereijido, M., E.S. Robbins, W.J. Dolan, C.A. Rotunno, and D.D. Sabatini. 1978. Polarized monolayers formed by epithelial cells on a permeable and translucent support. *J. Cell Biol.* 77:853–880.

Cohen, D., and A. Musch. 2003. Apical surface formation in MDCK cells: regulation by the serine/threonine kinase EMK1. *Methods.* 30:269–276.

Doyonnas, R., D.B. Kershaw, C. Duhme, H. Merkens, S. Chelliah, T. Graf, and K.M. McNagny. 2001. Anuria, omphalocele, and perinatal lethality in mice lacking the CD34-related protein podocalyxin. *J. Exp. Med.* 194:13–27.

Drubin, D.G., and W.J. Nelson. 1996. Origins of cell polarity. *Cell.* 84:335–344.

Füllekrug, J., P. Scheiffele, and K. Simons. 1999. VIP36 localisation to the early secretory pathway. *J. Cell Sci.* 112:2813–2821.

Grindstaff, K.K., C. Yeaman, N. Anandasabapathy, S.C. Hsu, E. Rodriguez-Boulan, R.H. Scheller, and W.J. Nelson. 1998. Sec6/8 complex is recruited to cell-cell contacts and specifies transport vesicle delivery to the basal-lateral membrane in epithelial cells. *Cell.* 93:731–740.

Gumbiner, B., and K. Simons. 1986. A functional assay for proteins involved in establishing an epithelial occluding barrier: identification of a uvomorulin-like polypeptide. *J. Cell Biol.* 102:457–468.

Horvat, R., A. Hovorka, G. Dekan, H. Poczewski, and D. Kerjaschki. 1986. Endothelial cell membranes contain podocalyxin—the major sialoprotein of visceral glomerular epithelial cells. *J. Cell Biol.* 102:484–491.

Hurd, T.W., L. Gao, M.H. Roh, I.G. Macara, and B. Margolis. 2003. Direct interaction of two polarity complexes implicated in epithelial tight junction assembly. *Nat. Cell Biol.* 5:137–142.

Ingber, D.E. 2003a. Tensegrity I. Cell structure and hierarchical systems biology. *J. Cell Sci.* 116:1157–1173.

Ingber, D.E. 2003b. Tensegrity II. How structural networks influence cellular information processing networks. *J. Cell Sci.* 116:1397–1408.

Keller, P., D. Toomre, E. Diaz, J. White, and K. Simons. 2001. Multicolour imaging of post-Golgi sorting and trafficking in live cells. *Nat. Cell Biol.* 3:140–149.

Kerjaschki, D., D.J. Sharkey, and M.G. Farquhar. 1984. Identification and char-

acterization of podocalyxin—the major sialoprotein of the renal glomerular epithelial cell. *J. Cell Biol.* 98:1591–1596.

Kerosuo, L., E. Juvonen, R. Alitalo, M. Gylling, D. Kerjaschki, and A. Miettinen. 2004. Podocalyxin in human haematopoietic cells. *Br. J. Haematol.* 124:809–818.

Kershaw, D.B., P.E. Thomas, B.L. Wharram, M. Goyal, J.E. Wiggins, C.I. Whiteside, and R.C. Wiggins. 1995. Molecular cloning, expression, and characterization of podocalyxin-like protein 1 from rabbit as a transmembrane protein of glomerular podocytes and vascular endothelium. *J. Biol. Chem.* 270:29439–29446.

Kershaw, D.B., S.G. Beck, B.L. Wharram, J.E. Wiggins, M. Goyal, P.E. Thomas, and R.C. Wiggins. 1997. Molecular cloning and characterization of human podocalyxin-like protein. Orthologous relationship to rabbit PCLP1 and rat podocalyxin. *J. Biol. Chem.* 272:15708–15714.

Kreitzer, G., J. Schmoranzer, S.H. Low, X. Li, Y. Gan, T. Weimbs, S.M. Simon, and E. Rodriguez-Boulan. 2003. Three-dimensional analysis of post-Golgi carrier exocytosis in epithelial cells. *Nat. Cell Biol.* 5:126–136.

Le Gall, A.H., C. Yeaman, A. Muesch, and E. Rodriguez-Boulan. 1995. Epithelial cell polarity: new perspectives. *Semin. Nephrol.* 15:272–284.

Lecuit, T., and E. Wieschaus. 2000. Polarized insertion of new membrane from a cytoplasmic reservoir during cleavage of the *Drosophila* embryo. *J. Cell Biol.* 150:849–860.

Li, Y., J. Li, S.W. Straight, and D.B. Kershaw. 2002. PDZ domain-mediated interaction of rabbit podocalyxin and Na^+/H^+ exchange regulatory factor-2. *Am. J. Physiol. Renal Physiol.* 282:F1129–F1139.

Matter, K., and I. Mellman. 1994. Mechanisms of cell polarity: sorting and transport in epithelial cells. *Curr. Opin. Cell Biol.* 6:545–554.

Mellman, I., and G. Warren. 2000. The road taken: past and future foundations of membrane traffic. *Cell.* 100:99–112.

Mostov, K., T. Su, and M. Ter Beest. 2003. Polarized epithelial membrane traffic: conservation and plasticity. *Nat. Cell Biol.* 5:287–293.

Nelson, W.J. 2003. Adaptation of core mechanisms to generate cell polarity. *Nature.* 422:766–774.

Nourry, C., S.G. Grant, and J.P. Borg. 2003. PDZ domain proteins: plug and play! *Sci STKE.* 2003:RE7.

Ojakian, G.K., and R. Schwimmer. 1988. The polarized distribution of an apical cell surface glycoprotein is maintained by interactions with the cytoskeleton of Madin-Darby canine kidney cells. *J. Cell Biol.* 107:2377–2387.

Ojakian, G.K., R. Schwimmer, and R.E. Herz. 1990. Polarized insertion of an intracellular glycoprotein pool into the apical membrane of MDCK cells. *Am. J. Physiol.* 258:C390–C398.

Ojakian, G.K., W.J. Nelson, and K.A. Beck. 1997. Mechanisms for de novo biogenesis of an apical membrane compartment in groups of simple epithelial cells surrounded by extracellular matrix. *J. Cell Sci.* 110:2781–2794.

Orlando, R.A., T. Takeda, B. Zak, S. Schmieder, V.M. Benoit, T. McQuistan, H. Furthmayr, and M.G. Farquhar. 2001. The glomerular epithelial cell anti-adhesin podocalyxin associates with the actin cytoskeleton through interactions with ezrin. *J. Am. Soc. Nephrol.* 12:1589–1598.

Ostedgaard, L.S., C. Randak, T. Rokhlina, P. Karp, D. Vermeer, K.J. Ashbourne Excoffon, and M.J. Welsh. 2003. Effects of C-terminal deletions on cystic fibrosis transmembrane conductance regulator function in cystic fibrosis airway epithelia. *Proc. Natl. Acad. Sci. USA.* 100:1937–1942.

Pazour, G.J., and G.B. Witman. 2003. The vertebrate primary cilium is a sensory organelle. *Curr. Opin. Cell Biol.* 15:105–110.

Pollack, A.L., R.B. Runyan, and K.E. Mostov. 1998. Morphogenetic mechanisms of epithelial tubulogenesis: MDCK cell polarity is transiently rearranged without loss of cell-cell contact during scatter factor/hepatocyte growth factor-induced tubulogenesis. *Dev. Biol.* 204:64–79.

Rodriguez-Boulan, E., K.T. Paskiet, and D.D. Sabatini. 1983. Assembly of enveloped viruses in Madin-Darby canine kidney cells: polarized budding from single attached cells and from clusters of cells in suspension. *J. Cell Biol.* 96:866–874.

Roh, M.H., and B. Margolis. 2003. Composition and function of PDZ protein complexes during cell polarization. *Am. J. Physiol. Renal Physiol.* 285:F377–F387.

Roh, M.H., S. Fan, C.J. Liu, and B. Margolis. 2003. The Crumbs3-Pals1 complex participates in the establishment of polarity in mammalian epithelial cells. *J. Cell Sci.* 116:2895–2906.

Saotome, I., M. Curto, and A.I. McClatchey. 2004. Ezrin is essential for epithelial organization and villus morphogenesis in the developing intestine. *Dev. Cell.* 6:855–864.

Schmieder, S., M. Nagai, R.A. Orlando, T. Takeda, and M.G. Farquhar. 2004. Podocalyxin activates RhoA and induces actin reorganization through NHERF1 and Ezrin in MDCK cells. *J. Am. Soc. Nephrol.* 15:2289–2298.

Schuck, S., A. Manninen, M. Honsho, J. Fullekrug, and K. Simons. 2004. Generation of single and double knockdowns in polarized epithelial cells by retrovirus-mediated RNA interference. *Proc. Natl. Acad. Sci. USA.* 101:4912–4917.

Shenolikar, S., and E.J. Weinman. 2001. NHERF: targeting and trafficking membrane proteins. *Am. J. Physiol. Renal Physiol.* 280:F389–F395.

Swiatecka-Urban, A., M. Duhaime, B. Coutermarsh, K.H. Karlson, J. Collawn, M. Milewski, G.R. Cutting, W.B. Guggino, G. Langford, and B.A. Stanton. 2002. PDZ domain interaction controls the endocytic recycling of the cystic fibrosis transmembrane conductance regulator. *J. Biol. Chem.* 277:40099–40105.

Takeda, T., W.Y. Go, R.A. Orlando, and M.G. Farquhar. 2000. Expression of podocalyxin inhibits cell-cell adhesion and modifies junctional properties in Madin-Darby canine kidney cells. *Mol. Biol. Cell.* 11:3219–3232.

Takeda, T., T. McQuistan, R.A. Orlando, and M.G. Farquhar. 2001. Loss of glomerular foot processes is associated with uncoupling of podocalyxin from the actin cytoskeleton. *J. Clin. Invest.* 108:289–301.

Takeuchi, K., K. Sakurada, H. Endou, M. Obinata, and M.P. Quinlan. 2002. Differential effects of DNA tumor virus genes on the expression profiles, differentiation, and morphogenetic reprogramming potential of epithelial cells. *Virology.* 300:8–19.

Verkade, P., T. Harder, F. Lafont, and K. Simons. 2000. Induction of caveolae in the apical plasma membrane of Madin-Darby canine kidney cells. *J. Cell Biol.* 148:727–739.

Voltz, J.W., E.J. Weinman, and S. Shenolikar. 2001. Expanding the role of NHERF, a PDZ-domain containing protein adapter, to growth regulation. *Oncogene.* 20:6309–6314.

Wang, A.Z., G.K. Ojakian, and W.J. Nelson. 1990. Steps in the morphogenesis of a polarized epithelium. I. Uncoupling the roles of cell-cell and cell-substratum contact in establishing plasma membrane polarity in multicellular epithelial (MDCK) cysts. *J. Cell Sci.* 95:137–151.

Yeaman, C., K.K. Grindstaff, M.D. Hansen, and W.J. Nelson. 1999. Cell polarity: versatile scaffolds keep things in place. *Curr. Biol.* 9:R515–R517.